JOURNAL OF MATERIALS SCIENCE 31 (1996) 4991–4995

Mechanical properties of sinter-forged Al_2O_3–ZrO_2 ceramics

J. KISHINO, A. NISHIYAMA
Central Research Institute, Mitsubishi Materials Co. Ltd, 1-297 Kitabukuro, Ohmiya-shi, Saitama 335, Japan

T. SAKUMA
Department of Materials Science, Faculty of Engineering, The University of Tokyo, 7-3-1 Hongo, Tokyo 113, Japan

Two kinds of composites, Al_2O_3–25 wt% ZrO_2(2 mol% Y_2O_3) (Y-ZTA), Al_2O_3–25 wt% ZrO_2(8 mol% CeO_2) (Ce-ZTA) were produced by the sinter-forging process. The effect of presintering temperature on the mechanical properties of the composites was examined. The sinter-forging process increased the room-temperature bending strength in comparison with pressureless sintering, owing to the smaller grain size in sinter-forged bodies than in pressureless sintered ones. It was found necessary to keep the presintering temperature considerably lower than sinter-forging temperature in order to improve the room-temperature strength. The strength of sinter-forged Ce-ZTA was higher than that of sinter-forged Y-ZTA. The residual surface compressive stress induced by the phase transition during grinding in Ce-ZTA was found to be effective to further improve the strength and fracture toughness.

1. Introduction

Much attention has been paid to zirconia-toughened alumina (ZTA) ceramics with high bending strength and fracture toughness at room temperature [1–4]. Some workers have reported that the bending strength of ZTA was improved by using hot isostatic pressing [2–4]. According to a recent report [5], the maximum bending strength of hot isostatically pressed (HIPed) ZTA was found to be up to 3 GPa for the TZP-based composites (Y-TZP/40 wt % Al_2O_3) and about 1 GPa for the Al_2O_3-based composites (Y-TZP/80 wt % Al_2O_3) [5].

In recent years, the superplastic sinter-forging process has been presented as a useful process to obtain sintered bodies with excellent mechanical properties [6]. This process has already been applied to ZrO_2 ceramics by some workers [7, 8]. Because ZTA ceramics show superplasticity at high temperatures, the sinter-forging may be applicable to improve their mechanical properties as well as ZrO_2 ceramics [9–12]. In sinter-forging, the sample is in a uniaxial stress condition, and is free of lateral constraint by the die wall. Thus a large shear strain can be imposed in sinter-forged materials. In this respect, sinter-forging is different from pressureless sintering and HIPing processes, where the shear strain is not applied. Venkatachari and Raj reported that the shear strain promotes the densification, suppresses the grain growth and then improves the mechanical properties [6].

In the present work, the effect of the sinter-forging process on the mechanical properties of ZTA was examined after the process had been evaluated. Among the various sinter-forging conditions, such as forging temperature, pressure, time, presintering temperature, etc., the effects of presintering temperature and of stabilizer (2 mol % Y_2O_3 or 8 mol % CeO_2) added to ZrO_2 on the bending strength of sinter-forged bodies were examined.

2. Experimental procedure

The starting materials used were high-purity alumina powders (Taimei Chemical Co. Ltd), and zirconia powders containing 2 mol % Y_2O_3 (Tosoh Co. Ltd) or 8 mol % CeO_2 (Osaka Cement Co. Ltd). Two kinds of composites, Al_2O_3–25 wt % ZrO_2 (2 mol % Y_2O_3) (Y-ZTA) and Al_2O_3–25 wt % ZrO_2 (8 mol % CeO_2) (Ce-ZTA), were prepared from the starting materials. Alumina and zirconia powders were ball-milled for 5 h in ethanol using high-purity zirconia balls. They were dried, sieved, and pressed under a pressure of 30 MPa in a cemented carbide die, and finally cold isostatically pressed under 150 MPa in a rubber tube. Presintering was performed at a temperature between 1100 and 1450 °C for 2 h. Rectangular samples with 16×16 mm^2 cross-section and 10 mm height were cut from the presintered bodies. They were sinter-forged under a uniaxial compressive stress of 50 MPa at 1400 °C for 1 h in air. The sinter-forging conditions were chosen by taking into account the conditions for superplastic flow of Al_2O_3–ZrO_2 ceramics [12]. The bulk density was measured by Archimedes' technique. The grain size was measured by a linear intercept

0022–2461

TABLE I Relative density of as-sintered and sinter-forged bodies

Presintering temperature (° C)	Relative density (%)			
	Y-ZTA		Ce-ZTA	
	As-sintered	Sinter-forged	As-sintered	Sinter-forged
1100	54.7	99.1	55.6	99.2
1200	59.7	99.0	–	–
1300	72.2	99.3	69.5	99.1
1350	84.7	99.3	87.0	99.2
1450	99.5	99.6	99.5	99.5

method using photographs taken with a Hitachi S-800 SEM. Thin foils prepared by ion milling were examined by transmission electron microscopy (TEM) using a Philipps CM-20 operated at 200 kV. Residual stress was measured by the X-ray diffraction method. The fracture strength was measured in a three-point bending test with specimens of dimensions $3 \times 4 \times 20\ mm^3$. The test jig had a span of 10 mm. The surfaces of the specimens were finished with 1 μm diamond paste. The tests were carried out at room temperature using an Instron-type mechanical testing machine at a crosshead speed of $0.5\ mm\ min^{-1}$. Fracture toughness was measured by the indentation microfracture method (IM).

3. Results and discussion

Table I shows the density of presintered and sinter-forged samples. The density of presintered bodies increased with increasing presintering temperature. Regardless of presintering temperatures, all samples sinter-forged at 1400 °C were almost fully dense.

The average size of ZrO_2 and Al_2O_3 grains in sinter-forged Al_2O_3–ZrO_2 is plotted as a function of presintering temperature in Fig. 1. The average grain size of Al_2O_3 and ZrO_2 decreases with decreasing presintering temperature. Compared with the average grain size of as-sintered bodies at 1450 °C, sinter-forged bodies have a small grain size if the presintering temperature is lower than the sinter-forging temperature. The grain growth is inhibited during the sinter-forging process in presintered samples.

Fig. 2 shows a transmission electron micrograph of as-sintered Y-ZTA. The dark and bright grains are ZrO_2 and Al_2O_3 grains, respectively. The ZrO_2 grains are located at grain-boundary corners of Al_2O_3. A transmission electron micrograph of a sinter-forged Y-ZTA is shown in Fig. 3. Grains are nearly equiaxed and no pores are observed. Dislocations are introduced in some Al_2O_3 grains after sinter-forging. The microstructures in as-sintered and sinter-forged Ce-ZTA are almost the same with those in Y-ZTA.

The bending strength and fracture toughness, K_{IC}, measured at room temperature are shown in Table II. The bending strength is plotted against presintering temperature in Fig. 4. The bending strength of sinter-forged bodies increased with a decrease of presintering temperature in Ce-ZTA and Y-ZTA. In particular, the strength of sinter-forged Ce-ZTA

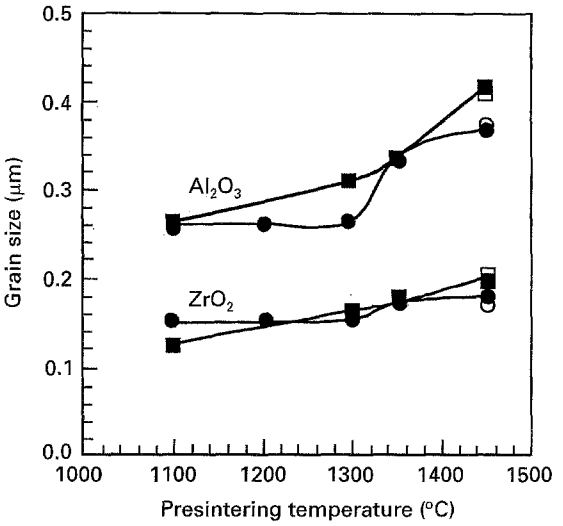

Figure 1 The relation between grain size of Al_2O_3 and ZrO_2 and presintering temperature in sinter-forged and as-sintered bodies. The as-sintered Ce-ZTA and Y-ZTA were obtained by sintering at 1450 °C for 2 h. (■) Sinter-forged Ce-ZTA, (●) sinter-forged Y-ZTA, (□) as-sintered Ce-ZTA, (○) as-sintered Y-ZTA.

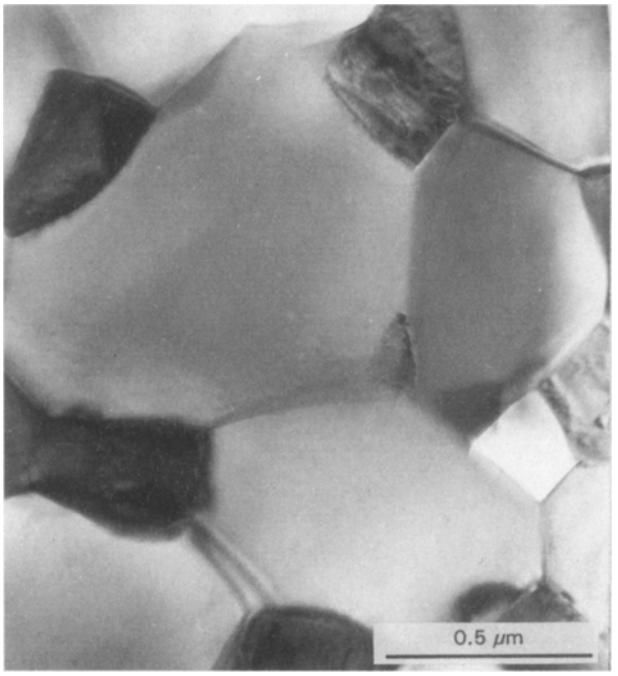

Figure 2 Transmission electron micrograph of as-sintered sample at 1450 °C in Y-ZTA.

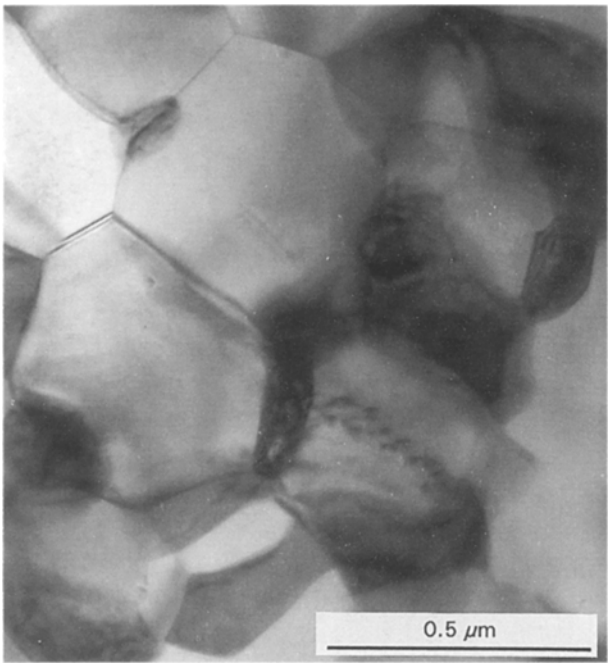

Figure 3 Transmission electron micrograph of the sinter-forged sample in Y-ZTA. Presintering temperature is 1300 °C.

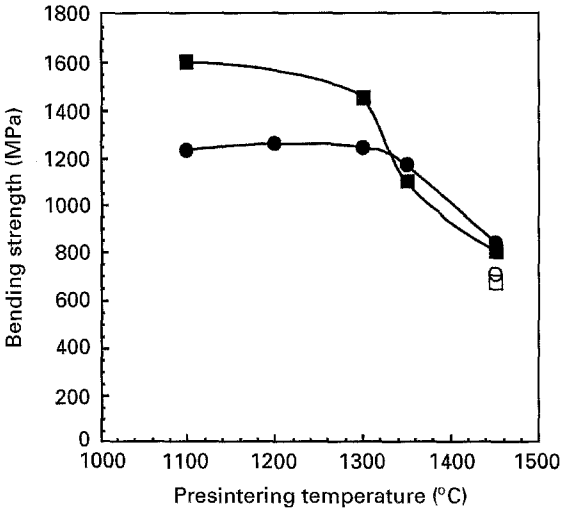

Figure 4 A plot of bending strength as a function of presintering temperature in sinter-forged and as-sintered bodies in Y-ZTA and Ce-ZTA. (■) Sinter-forged Ce-ZTA, (●) sinter-forged Y-ZTA, (□) as-sintered Ce-ZTA, (○) as-sintered Y-ZTA.

presintered at 1100 °C was as high as 1.6 GPa. In contrast, the strength of sinter-forged Y-ZTA was not as high as that of Ce-ZTA at presintering temperatures below 1300 °C and was nearly constant (about 1.2 GPa) at presintering temperatures between 1100 and 1300 °C. An interesting fact is that the sinter-forging is not effective to increase the strength of samples presintered at 1450 °C.

The relation between the bending strength and average size of Al_2O_3 and ZrO_2 grains is shown in Fig. 5. A linear relation is obtained between the strength and the inverse square root of ZrO_2 or Al_2O_3 grain size, $d^{-1/2}$, in Y-ZTA. The solid lines drawn for the data of Y-ZTA were calculated using a least squares method. The strength of sinter-forged Ce-ZTA deviate slightly from the linear relation in the fine grain-size region. This figure shows that the higher strength of sinter-forged materials is due to the finer grain size. However, the difference in strength between Y-ZTA and Ce-ZTA cannot be explained by the finer grain-size effect alone. The difference is also caused by the stability of tetragonal zirconia.

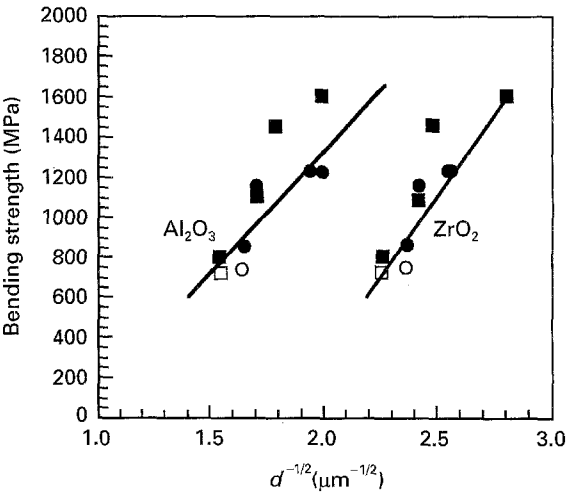

Figure 5 The relation between bending strength and average grain size of Al_2O_3 and ZrO_2 in sinter-forged Y-ZTA and Ce-ZTA. (■) Sinter-forged Ce-ZTA, (●) sinter-forged Y-ZTA, (□) as-sintered Ce-ZTA, (○) as-sintered Y-ZTA.

The proportion of tetragonal and monoclinic ZrO_2 was determined from X-ray diffraction data using CuK_α radiation by measuring the relative intensities of monoclinic and tetragonal reflections [13]. The

TABLE II Mechanical properties of sinter-forged bodies

	Y-ZTA		Ce-ZTA	
Presintering temperature (° C)	Bending strength (MPa)	K_{IC} (MPa m$^{1/2}$)	Bending strength (MPa)	K_{IC} (MPa m$^{1/2}$)
1100	1235	4.1	1610	7.8
1200	1264	4.3	–	–
1300	1247	3.9	1445	5.9
1350	1170	3.8	1104	4.3
1450	838	3.9	800	4.4
1450 (pressureless sintered)	704	4.1	686	4.4

percentage of monoclinic ZrO_2 (m-ZrO_2) was determined by

$$\text{vol}\,\%\ \text{m-}ZrO_2 = \{I_m(1\,1\,\bar{1}) + I_m(1\,1\,1)\}/\{I_m(1\,1\,1) + I_m(1\,1\,\bar{1}) + I_t(1\,1\,1)\} \times 100 \quad (1)$$

where $I_m(1\,1\,1)$ and $I_m(1\,1\,\bar{1})$ are intensities of m-ZrO_2 from the (1 1 1) and (1 1 $\bar{1}$) planes, and $I_t(1\,1\,1)$ is the intensity of tetragonal zirconia (t-ZrO_2) from the {1 1 1} plane.

The presence of m-ZrO_2 was only detected in the ground surface of sinter-forged Ce-ZTA, and not found in sinter-forged Y-ZTA even in the ground surface. The volume fraction of m-ZrO_2 is shown as a function of presintering temperature in Fig. 6. Because m-ZrO_2 does not exist in sinter-forged samples, the transformation from t-ZrO_2 to the m-ZrO_2 must be induced during grinding of the sinter-forged Ce-ZTA. The t-ZrO_2 in sinter-forged Ce-ZTA is unstable in comparison with sinter-forged Y-ZTA. As shown in Fig. 6, the m-ZrO_2 fraction of sinter-forged Ce-ZTA increases with decreasing presintering temperature. The stability of t-ZrO_2 is dependent on presintering temperature.

Because the transformation involves a volume increase, the compressive residual stress is generated in the surface layer of sinter-forged and ground Ce-ZTA. Assuming that the ground surface is regarded as a thin layer on a substrate, the compressive biaxial surface stress, σ_s, in the transformed layer can be approximated by [14]

$$\sigma_s = 1/3(\Delta V/V)EV_i/(1 - \nu) \quad (2)$$

where $\Delta V/V$ is the fractional molar volume increase associated with the transformation, V_i is the volume fraction of material with an increased molar volume, E is the Young's modulus, and ν is the Poisson's ratio.

Fig. 7 shows the comparison between surface compressive stress measured by X-ray analysis and that calculated from Equation 2 as a function of presintering temperature. The experimental and calculated residual stresses agree fairly well with each other.

The strengthening due to compressive surface stress has been studied by several investigators [15–20]. It has been shown that the ceramics containing t-ZrO_2 dispersion become strong by surface grinding [16–20]. For example, Claussen and co-workers showed that the ground Al_2O_3–ZrO_2 is twice as strong as the annealed one [18, 19]. It seems reasonable that the surface compressive stress is an origin of higher bending strength of Ce-ZTA than that of Y-ZTA at presintering temperature below 1300 °C (Table II). In addition, the fracture toughness, K_{IC}, is higher in Ce-ZTA than in Y-ZTA as seen in Table II. K_{IC} measured by the IM technique is known to be influenced by surface residual compressive stress [21]. The high K_{IC} value in Ce-ZTA in comparison with Y-ZTA must also be associated with surface compressive stress.

Another interesting fact is that the tetragonal to monoclinic phase transition is only induced in Ce-ZTA during grinding but not in Y-ZTA. According to Tsukuma and Shimada [22], t-ZrO_2 in Ce-TZP exhibits better thermal stability than that in Y-TZP

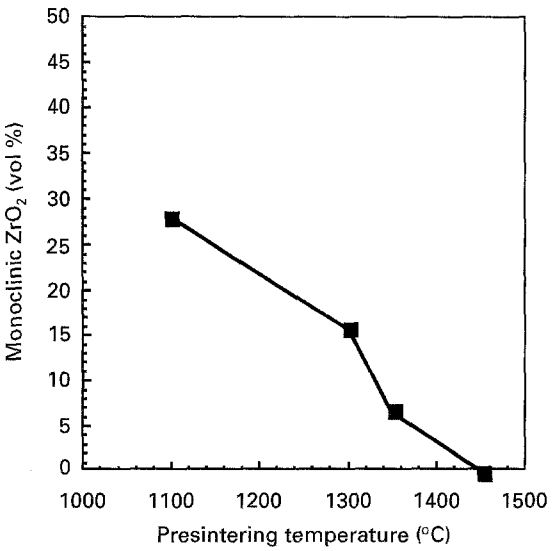

Figure 6 The volume percentage of monoclinic ZrO_2 in sinter-forged Ce-ZTA as a function of presintering temperature.

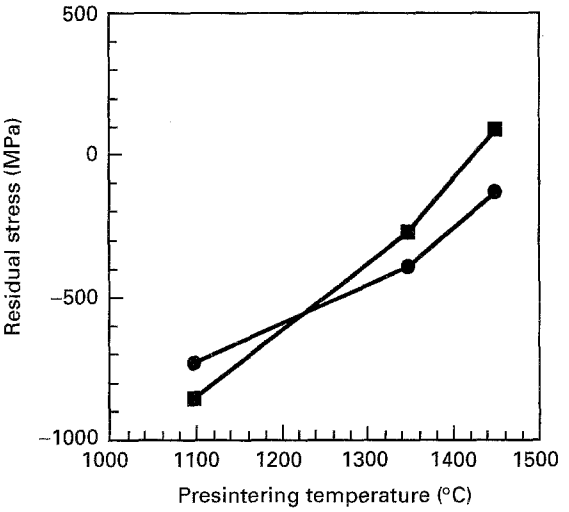

Figure 7 The surface compressive stress measured by X-ray diffraction analysis and calculated from Equation 2 as a function of presintering temperature in sinter-forged Ce-ZTA. (■) Experimental data, (●) calculated data.

under thermal cycling or hydrothermal conditions, and the stability of t-ZrO_2 in Ce-TZP increases with decreasing grain size. The present result is inconsistent with their result. The reason for the difference is not clear at present. The present results show that t-ZrO_2 in sinter-forged Ce-ZTA is more easily transformed into m-ZrO_2 than that in simply compressed bodies or pressureless-sintered ones. The sinter-forging process may influence the stability of t-ZrO_2 in Ce-ZTA.

4. Conclusions

Al_2O_3–25 wt % ZrO_2 (2 mol % Y_2O_3 or 8 mol % CeO_2) composites (Y-ZTA, Ce-ZTA) were produced by sinter-forging, and their mechanical properties were examined. The results obtained are summarized as follows.

1. The room-temperature bending strength of sinter-forged bodies is higher than that of pressurelessly

sintered ones, especially in sinter-forged Ce-ZTA. The strength of sinter-forged Ce-ZTA increases with decreasing presintering temperature.

2. The transformation of t-ZrO_2 into m-ZrO_2 is induced by grinding in sinter-forged Ce-ZTA, but not in pressurelessly sintered Ce-ZTA and sinter-forged Y-ZTA.

3. The improvement of strength due to sinter-forging is explained by grain-size refinement. In addition, the residual surface compressive stress caused by stress-induced phase transformation by grinding in sinter-forged Ce-ZTA is effective to improve the bending strength and fracture toughness.

References

1. F. F. LANGE, *J. Mater. Sci.* **17** (1982) 247.
2. K. TSUKUMA, K. UEDA and M. SHIMADA, *J. Am. Ceram. Soc.* **68** (1985) C4.
3. S. HORI, M. YOSHIMURA and S. SOMIYA, *ibid.* **69** (1986) 169.
4. D-W. SHIN, K. K. ORR and H. SCHUBERT, *ibid.* **73** (1990) 1181.
5. R. SHIKATA, T. YAMAMOTO, T. SHIONO and T. NISHIKAWA, *J. Jpn Soc. Powder Powder Metall.* **37** (1990) 357.
6. K. R. VENKATACHARI and R. RAJ, *J. Am. Ceram. Soc.* **70** (1987) 514.
7. P. C. PANDA, J. WANG and R. RAJ, *ibid.* **71** (1988) C504.
8. I. A. AKMOULIN, M. DJAHAZI, N. D. BURAVOVA and J. J. JONAS, *Mater. Sci. Technol.* **9** (1993) 26.
9. F. WAKAI and H. KATO, *Adv. Ceram. Mater.* **3** (1988) 71.
10. R. MARTIENZ, R. DUCLOS and J. CRAMPON, *ibid.* **24** (1990) 1979.
11. A. H. CHOKSHI, T-G. NIEH and J. WADSWORTH, *J. Am. Ceram. Soc.* **74** (1991) 869.
12. K. OKADA, Y. YOSHIZAWA and T. SAKUMA, in "Superplasticity in Advanced Materials", edited by S. Hori, M. Tokizane and N. Furushiro (Japan Society for Research on Superplasticity, Osaka, 1991) p. 227.
13. R. C. GARVIE and P. S. NICHOLSON, *J. Am. Ceram. Soc.* **55** (1972) 303.
14. D. J. GREEN, F. F. LANGE and R. JAMES, *ibid.* **66** (1983) 623.
15. J. S. REED and A. LEJUS, *Mater. Res. Bull.* **12** (1977) 949.
16. D. J. GREEN and F. F. LANGE, *Am. Ceram. Soc. Bull.* **58** (1979) 883.
17. T. K. GUPTA, *J. Am. Ceram. Soc.* **63** (1980) 117.
18. N. CLAUSSEN and G. PETZOW, in "Energy and Ceramics", edited by P. Vincenzini (Elsevier, Amsterdam, 1980) p. 680.
19. N. CLAUSSEN and M. RUHLE, in "Advances in Ceramics", Vol. 3, edited by A. H. Heuer and L. W. Hobbs (American Ceramic Society, Columbus, OH, 1981) p. 137
20. T. KOSMAC, R. WAGNER and N. CLAUSSEN, *J. Am. Ceram. Soc.* **64** (1981) C72.
21. S. HORI, M. YOSHIMURA, R. KURITA, H. KAJI and S. SOMIYA, *J. Ceram. Soc. Jpn* **92** (1984) 296.
22. K. TSUKUMA and M. SHIMADA, *J. Mater. Sci.* **20** (1985) 1178.

Received 18 May 1994
and accepted 13 February 1996